Available online at www.sciencedirect.com
ScienceDirect
Trans. Nonferrous Met. Soc. China 25(2015) 2342−2351
Transactions of Nonferrous Metals Society of China
www.tnmsc.cn

Effect of friction coefficient in deep drawing of AA6111 sheet at elevated temperatures

Wen-yu MA[1], Bao-yu WANG[1], Lei FU[2], Jing ZHOU[1], Ming-dong HUANG[1]

1. School of Mechanical Engineering, University of Science and Technology Beijing, Beijing 100083, China;
2. Suzhou Institute for Non-ferrous Metal Research, Suzhou 215026, China

Received 24 September 2014; accepted 28 November 2014

Abstract: The effect of friction coefficient on the deep drawing of aluminum alloy AA6111 at elevated temperatures was analyzed based on the three conditions using the finite element analysis and the experimental approach. Results indicate that the friction coefficient and lubrication position significantly influence the minimum thickness, the thickness deviation and the failure mode of the formed parts. During the hot forming process, the failure modes are draw mode, stretch mode and equi-biaxial stretch mode induced by different lubrication conditions. In terms of formability, the optimal value of friction coefficient determined in this work is 0.15. At the same time, the good agreement is performed between the experimental and simulated results. Fracture often occurs at the center of cup bottom or near the cup corner in a ductile mode or ductile−brittle mixed mode, respectively.

Key words: aluminum alloy; deep drawing; friction coefficient; formability; fracture surface

1 Introduction

Recently, the lightweight materials have been increasingly applied to automobile components traditionally made of steel in response for reducing fossil fuel consumption and environment protection [1−5]. Aluminum alloys have attracted considerable attention among many lightweight materials, because of their low density, high specific strength and good recyclability [6−8].

Aluminum alloy parts are generally cold formed; however, the ductility of aluminum alloys at room temperature is low, resulting in poor formability [9]. Compared with the cold forming, superplastic forming can achieve good formability with better forming accuracy in terms of geometric tolerance. However, the disadvantages of superplastic forming are low strain rate and strict requirement for specialized grain size of raw material, which are not reasonable for mass-produced parts [10,11]. Warm forming can improve the ductility of aluminum alloys at elevated temperatures in a short production cycle time; however, heating the tools and blank during the forming process adds the complexity of this technology [12,13]. By contrast, blank ductility is significantly enhanced in hot stamping of aluminum alloys, thus, more complex parts can be formed in one process [14,15]. The formed part is held within the dies for several seconds after deformation to obtain rapid quenching and avoid thermal distortion, and then, artificially aged for hardening. Hot stamping of aluminum alloys can improve the dimension accuracy and mechanical properties of the parts. This novel technology has received considerable interests recently [16,17].

In order to get a good formability in the aluminum alloy hot stamping, the effect of process parameters on forming characteristics should be investigated. In literatures, studies on deep drawing are often conducted to explore the influence of variables, such as friction coefficient, blank holder force and forming velocity.

BROWNE and HILLERY [18] studied the effects of forming factors, including lubrication type and lubrication position, on the drawing formability. Numerous experimental explorations and analyses were conducted and used to determine the importance level of

Foundation item: Project (2009ZX04014-074) supported by the National Science and Technology Major Project of China; Project (P2014-15) supported by the State Key Laboratory of Materials Processing and Die & Mould Technology, Huazhong University of Science and Technology, China; Project (20120006110017) supported by the Specialized Research Fund for the Doctoral Program of Higher Education of China
Corresponding author: Bao-yu WANG; Tel/Fax: +86-10-82375671; E-mail: bywang@ustb.edu.cn
DOI: 10.1016/S1003-6326(15)63849-3

different parameters on the wall thickness distribution and the punch load. PADMANABHAN et al [19] analyzed the influence of various process parameters on deep drawing. Results show that the percentage contribution of friction coefficient on average thickness is higher than that of the blank holder force. RAJU et al [20] conducted deep drawing tests to analyze the influence of variables, such as blank holder force, die shoulder radius and punch nose radius on the thickness distribution at room temperature. The optimum combination of these parameters was determined to get even thickness variation.

Great efforts have been devoted to analyzing the effects of process parameters on drawing characteristics. However, knowledge on the influences of process parameters on the deep drawing of aluminum alloys at elevated temperatures is limited. Especially the importance of friction coefficient on the forming characteristics, i.e., minimum thickness, thickness deviation and failure mode, is necessary to be analyzed. Then the new knowledge can be added into the fields. In order to study the effect of friction coefficient on formability, several kinds of commercial lubricants could be used in the experiments. Utilizing lubricants can exhibit various lubrication influences. Finite element analysis (FEA) was employed to analyze how the friction coefficient affects minimum thickness, thickness deviation and deformation mode of deep-drawing cups. The fracture surfaces of differently drawn cups were studied using scanning electron microscope (SEM) to get a further understanding.

2 Finite element model

Using the coupled thermal-mechanical axisymmetric deformation model, FEA of deep-drawing at elevated temperatures was conducted for aluminum alloy AA6111 according to the design of FE simulations. The FE model comprises four components: punch, blank, blank holder and die. Given the symmetry of this problem, a quarter of the model was built with the symmetry plane to save calculation time and computer memory. The schematic diagram of the coupled temperature−displacement model is shown in Fig. 1. The detailed dimensions of each component are illustrated in Table 1. The blank is modeled as deformable part meshed by four-node shell element, whereas other components are rigid bodies with thermal properties. The physical and thermal properties of materials used in the FE model are illustrated in Table 2 [21]. The heat transfer coefficients depending on the gap between the blank and tools and on the contact pressure are shown in Table 3 [22].

Aluminum alloy AA6111 belongs to Al−Mg−Si series alloys that can be strengthened by heat treatment and is mainly used in automobile manufacturing. The chemical composition of AA6111 is listed in Table 4. The blank was originally supplied in a large sheet from ALCOA Company with thickness of 2 mm in T4 condition. Dog-bone-shaped samples were cut from the large sheet with the parallel length of 60 mm and width

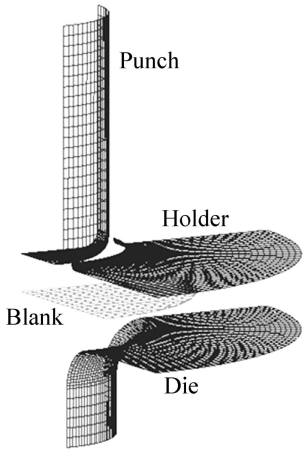

Fig. 1 Schematic diagram of coupled temperature−displacement model

Table 1 Dimensions of drawing tools

Punch diameter/mm	Punch corner radius/mm	Die diameter/mm	Die corner radius/mm	Blank thickness/mm	Blank diameter/mm
50	5	54.4	13	2	100

Table 2 Physical and thermal properties of materials used in FE model [21]

Property	Blank	Tools
Density, ρ/(g·cm^{-3})	2.7	7.8
Thermal conductivity, λ/(mW·mm^{-1}·K^{-1})	167	20
Specific heat, c/(J·g^{-1}·K)	9.2×10^5	6.5×10^5
Elasticity modulus, E/MPa	70000	−
Poisson ratio, v	0.3	−

Table 3 Heat transfer coefficients depending on gap and pressure [22]

Gap/mm	Pressure/MPa	Heat transfer coefficient/(mJ·mm^{-2}·s^{-1}·K^{-1})
1.45	−	0
0.6	−	0.07
0	0	0.3
0	5	0.345
0	15	1.424
0	25	1.518

of 12 mm. During the hot tensile tests, the blank deformed at elevated temperatures under various strain rates. In order to reveal the flow behavior, tensile tests were conducted over temperature range of 350−550 °C and strain rate range of 0.1−10 s^{-1} using a Gleeble 1500. The tensile stress−strain curves of AA6111 shown in Fig. 2 indicate that flow stress is sensitively dependent on the deformation temperature and the strain rate. The stress and strain relationships at other temperatures and strain rates can be interpolated from obtained experimental data.

Table 4 Chemical composition of AA6111aluminum alloy (mass fraction, %)

Si	Fe	Cu	Mn	Mg	Cr	Zn	Ti	Al
0.75	0.40	0.55	0.25	0.80	0.10	0.15	0.10	Bal.

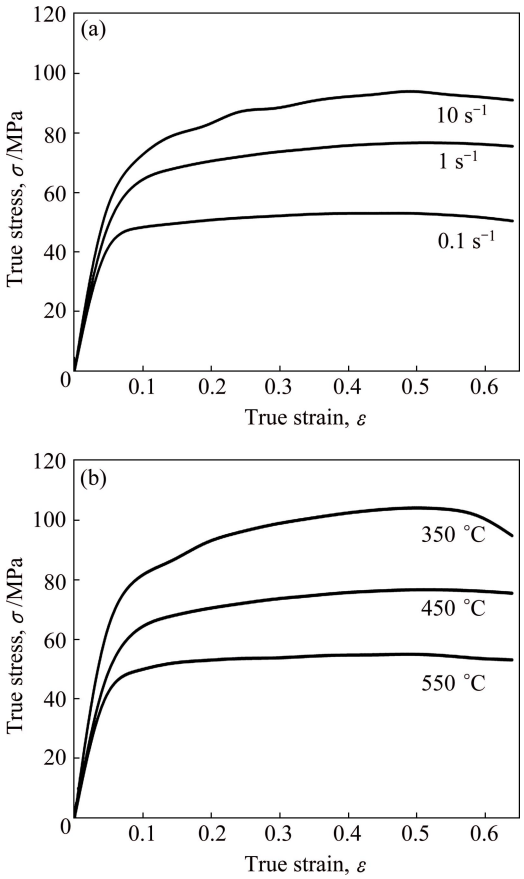

Fig. 2 True stress−true strain curves of AA6111 under different temperatures and various strain rates: (a) t=450 °C; (b) $\dot{\varepsilon}$=1 s^{-1}

3 Design of FE simulations

In this work, the effect of the friction coefficient ranging from 0 to 0.30 is evaluated. The friction coefficient range is chosen based on lubrication properties and work experience. Some lubricants, such as Dag 2404, Dag F-425 and other graphitic lubricants, are effective at elevated temperatures. In practice, the friction coefficient varies depending on many factors, such as deformation temperature, pressure and roughness distribution. YANAGIDA and AZUSHIMA [23] conducted the evaluation of friction coefficients in hot flat drawing process of SPHC steel and high strength steel. However, the related knowledge on aluminum alloys in hot forming is limited. In this FE model, the friction coefficient is assumed constant during hot forming process.

The study on friction coefficient effects is carried out under three conditions. Under condition 1, the friction coefficients for any interaction (such as the interactions between the blank and the punch, between the blank and the holder, and between the blank and the die) are the same and the friction coefficient is defined as μ_0; under condition 2, both the friction coefficient between the blank and the holder and that between the blank and the die are kept constant as 0.2, and the friction coefficient between the blank and the punch is defined as μ_1; under condition 3, the friction coefficient between the blank and the punch is kept constant as 0.2, the friction coefficient between the blank and the holder is defined as μ_2, at the same time, the friction coefficient between the blank and the die is also set as same as μ_2. For each condition, the friction coefficient varies from 0 to 0.3 at the interval of 0.05 or 0.10. The specific simulation designs under different conditions are shown in Table 5. In Table 5, "✓" indicates that the test is conducted for this specific value and "–" indicates that the test is not carried out for this specific value.

Table 5 Design of simulations under different conditions

Friction coefficient	0	0.05	0.10	0.15	0.25	0.30
μ_0	✓	✓	–	✓	✓	✓
μ_1	✓	✓	✓	✓	✓	✓
μ_2	✓	✓	–	✓	✓	✓

After determining the design of simulations, quality criteria should be chosen to measure the formability and determine the effect of process parameters. As there is no single criterion allowing for the global evaluation of all drawing processes, it is difficult to determine the formability [24]. PARK and KIM [25] have carried out simulations of deep drawing of steel sheet. The minimum thickness was used as forming quality index to measure effect of the process parameters on the formability. Results imply that the friction coefficient and the plastic anisotropy parameter significantly affect the deep drawing ability of steel sheets. JAISINGH et al [26] conducted sensitivity analysis of a deep drawing. The maximum thinning strain is employed as the quality characteristic. The blank holder force has the maximum

influence on the peak thinning strain followed by friction coefficient. In Ref. [27], the design of experiments and statistical analysis have been utilized to determine how the factors, such as punch radius, lubricant type and lubricant position affect the wall thickness deviation, which is developed to reflect forming quality. CHEN et al [28] have studied the formability of cup drawing by forming limit test. At the same time, the strain paths tracing crack points in the drawing process are recorded in the forming limit diagram (FLD) to determine the failure mode. The failure mode changes for different values of process parameter.

In the present work, FE simulations were carried out using initial blank temperature of 550 °C, initial tool temperature of 25 °C, punch velocity of 200 mm/s and blank holder force of 2000 N. After simulating the hot drawing process, the wall thickness variation of the formed cup at the stroke of 30 mm was recorded. The quality characteristics measured were the minimum thickness and the standard deviation from average thickness, which is defined as thickness deviation. At the same time, the strain paths tracing the fracture element during the deep drawing process under each condition were also recorded to measure the failure mode.

In real experiments, several types of high temperature resistant lubricants can be used to paint on the blank or the tools. The position and quantity of the lubricant used in experiments were based on different conditions. For example, in condition 1, the lubricant was only painted on both sides of the blank; in condition 2, the lubricant A was painted on both sides of the blank and lubricant B was painted on the punch face.

4 Results and discussion

In this work, the quality characteristics measured are the minimum thickness and the thickness deviation. In terms of minimum thickness, a larger minimum thickness is better. Generally, the maximum thinning rate should be no more than 20% for hot drawing [22]; thus, the minimum thickness of the formed part should be larger than 1.6 mm. And the thickness value lower than 1.6 mm indicates the occurrence of excessive thinning. With regard to thickness deviation, lower thickness deviation is better. The low thickness deviation indicates good evenness of the wall thickness distribution. The FLD and strain path of failure element are used to determine the deformation mode, namely, draw mode (i.e., the left-hand side of the FLD), plane strain mode (i.e., the minor strain is zero), stretch mode (i.e., the right-hand side of the FLD) and equi-biaxial stretch mode (i.e., the major strain is equal to the minor strain) and so on [28]. The identification of different failure modes during forming can contribute to furthering the understanding of deep drawing of aluminum alloys at elevated temperatures [24].

4.1 Effect of friction coefficient μ_0

Figure 3 illustrates the effect of friction coefficient μ_0 on thickness variation. In order to elaborate the thickness variation clearly, the formed part can be analyzed in five distinct regions. The schematic diagram for a formed cup is shown in Fig. 4.

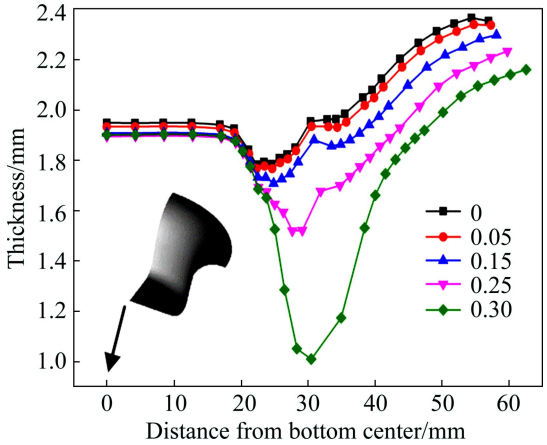

Fig. 3 Thickness distribution with various friction coefficients μ_0 under condition 1

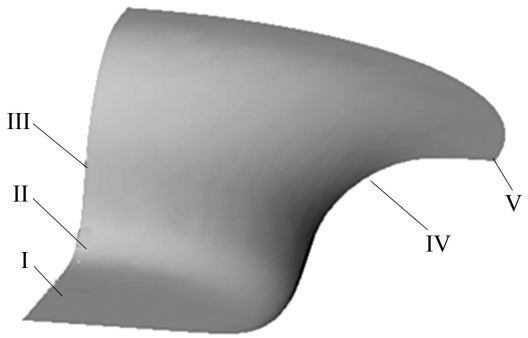

Fig. 4 Schematic diagram for cup regions: I—Cup bottom; II—Punch corner; III—Sidewall; IV—Die corner; V—Flange

As shown in Fig. 3, the thickness of cup bottom is not sensitive to friction coefficient μ_0 and the material of the cup bottom is subjected to biaxial tension and frictional stress. The friction force also restrains the blank from sliding past the punch corner.

Except for the cup bottom region, the thickness variation of other regions shows great dependency on the friction coefficient μ_0. Thickness significantly decreases as friction coefficient increases, especially at μ_0 larger than 0.15. As the friction coefficient μ_0 is 0.30, the minimum thickness happening near punch corner is smaller than 1.1 mm. Compared with other regions, the temperature of the material in the sidewall is slightly higher, which is attributed to lower heat transfer.

Heat transfer has three modes, namely conduction, convection and radiation. Conduction from hot blank to

cold tools mainly causes blank temperature reduction compared with convection and radiation from hot blank to environment. The heat flux from hot blank to cold tools strongly depends on the gap between the blank and the tools and the contact pressure. Given the presence of a gap between the punch and the die, the sidewall material has a certain distance from the tools, which decreases heat transfer. The blank area not in contact with the tools is hotter, thereby it demonstrates higher ductility and lower flow stress. Thus, the eventual excessive thinning is easy to initiate at the junction of the punch corner and the sidewall.

In the flange region, the blank is clamped between the holder and the die. When the blank slides forth, friction forces act on both sides of the blank depending on the friction coefficient and the contact pressure. Therefore, as the friction coefficient increases, the force needed to draw the material into the die cavity increases, which stretches the formed cup wall and causes uneven thickness variation. Near the edge of the flange, the material significantly thickens. Notably, the edge of the flange moves less into the die cavity with larger friction coefficient, resulting in the obvious elongation of the cup wall.

After analyzing the relationship between thickness distribution and friction coefficient, the minimum thickness and the thickness deviation calculated for each friction coefficient were recorded, as shown in Fig. 5.

In Fig. 5, the symbols are simulation results and smooth curves are used to reflect the variation trends of those results. The correlation equations of quality indexes and friction coefficients are obtained by exponential fitting using mathematical software. These equations are presented with the simulation results and they can be used to predict other results.

Figure 5(a) clearly illustrates that the minimum thickness decreases with increasing friction coefficient μ_0. When the friction coefficient μ_0 is larger than 0.15, the minimum thickness markedly decreases to be lower than 1.7 mm. When the friction coefficient is 0.30, the minimum thickness is about 1.01 mm and the thinning rate is 49.5%. This indicates the excessive thinning of the deep drawn part.

As shown in Fig. 5(b), the thickness deviation decreases as the friction coefficient μ_0 increases to less than 0.15, and then, thickness deviation increases as the friction coefficient μ_0 further increases. The lowest thickness deviation value of 0.17 mm is obtained at the friction coefficient μ_0 of 0.15, which indicates a relatively uniform thickness distribution. The largest thickness deviation value of 0.32 mm was obtained at the friction coefficient μ_0 of 0.30, which indicates a severely uneven thickness variation of the formed cup, resulting in bad formability.

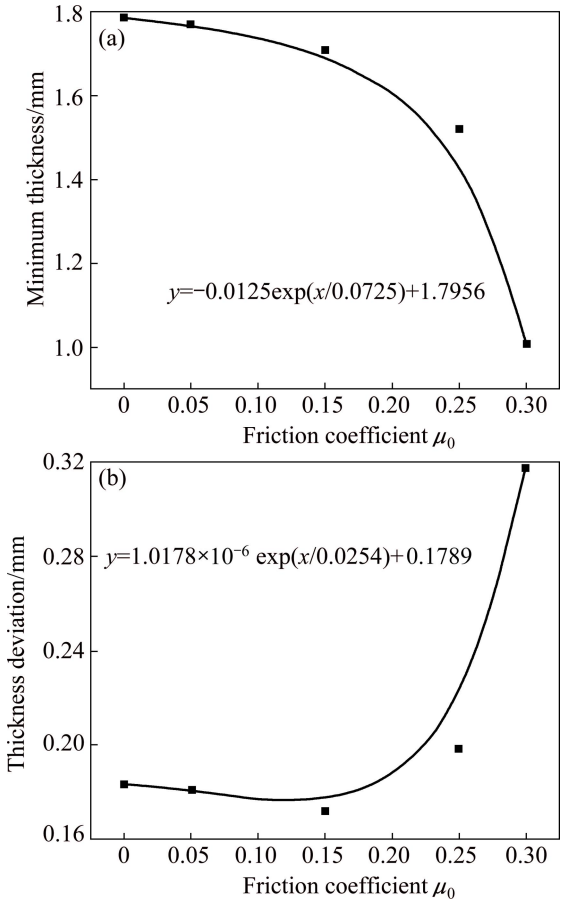

Fig. 5 Relationship between friction coefficient μ_0 and minimum thickness (a) and thickness deviation (b) under condition 1

The FLD and the strain path tracing the failure element are used in aluminum alloy forming analysis to further study deep drawing and to examine the failure mode when the blank is formed into cup shape by deep drawing at elevated temperatures. In Fig. 6, the strain path (dashed line) of excessive thinning element near the punch corner was obtained when the friction coefficient μ_0 is 0.30. The left Fig. 6 shown in is the real formed part. The black stains on the part are the marks of high temperature resistant lubricant. The forming limit curve (FLC) was derived from Ref. [29]. CHOW et al [29] used the model to predict the FLDs for 6111-T4 aluminum alloy. The analysis strategy of using the combination of FLC and strain path is based on the study of CHEN et al [28]. CHEN et al [28] have employed the FLC and strain path of failure element to analyze the effect of forming parameters. Figure 6 shows that the fracture element strains are in the stretch mode, i.e., the right-hand side of the FLD, at the start of drawing process and move toward the draw mode afterwards. However, the minor strain is relatively small compared with major strain, which indicates that the circumferential strain of the failure element near the

punch corner is small, at the same time, the material suffers large deformation in the radial direction. This is because the material in both flange and bottom regions is hard to supplement at large friction coefficient, thereby leading to the forming failure.

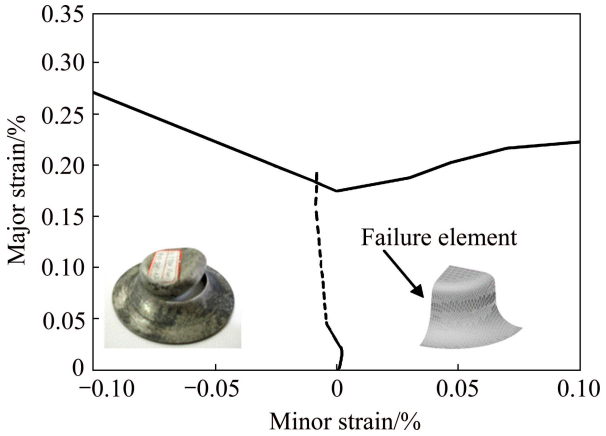

Fig. 6 Strain path of failure element under condition 1

4.2 Effect of friction coefficient μ_1

In this section, the friction coefficient between the blank and the punch is defined as μ_1 and the friction coefficient between the blank and the holder, and the die is kept constant as 0.20. The thickness distributions along the cup profile under various friction coefficients μ_1 are illustrated in Fig. 7.

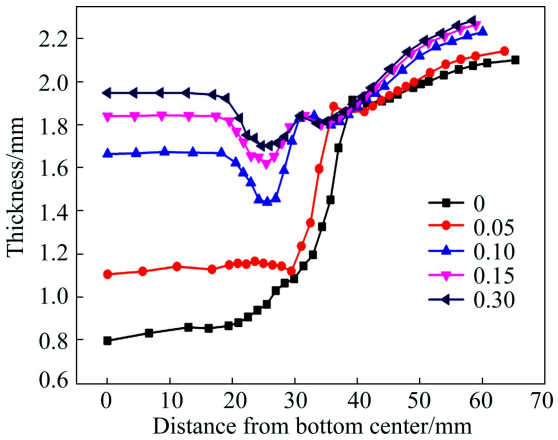

Fig. 7 Thickness distribution with various friction coefficients μ_1 under condition 2

As shown in Fig. 7, thickness reduction at the cup bottom is greatly sensitive to friction coefficient μ_1. Cup bottom thickness significantly reduces as friction coefficient μ_1 decreases, especially when the friction coefficient μ_1 is smaller than 0.15. The observation is attributed to friction force reduction, which was imposed on the blank from the punch face. Thus, the material easily slides over the punch corner. At a small friction coefficient μ_1, the small friction force imposed on the blank from punch face can lead to severe thinning at the bottom center. When the friction coefficient μ_1 is larger than 0.10, the maximum localized thinning still occurs near the corner of the cup. The flange thickness is observed to be less affected by friction coefficient μ_1. The elongation of the part increases with decreasing friction coefficient μ_1. This is because the friction force preventing the material from sliding over the punch corner is small when the friction coefficient μ_1 is small; thus, cup bottom deformation can easily happen. The force that drags the flange region material from sliding over the die corner also decreases, and the elongation of the part becomes more apparent as friction coefficient μ_1 decreases.

Figure 8(a) illustrates the relationship between the minimum thickness and the friction coefficient μ_1. The minimum thickness increases with increasing friction coefficient μ_1. When the friction coefficient μ_1 is 0, the minimum thickness is 0.8 mm. When the friction coefficient μ_1 is 0.30, the minimum thickness is 1.7 mm, indicating a successful drawing process. The minimum thickness increases significantly when the friction coefficient μ_1 is lower than 0.15, and then, the minimum thickness increases smoothly.

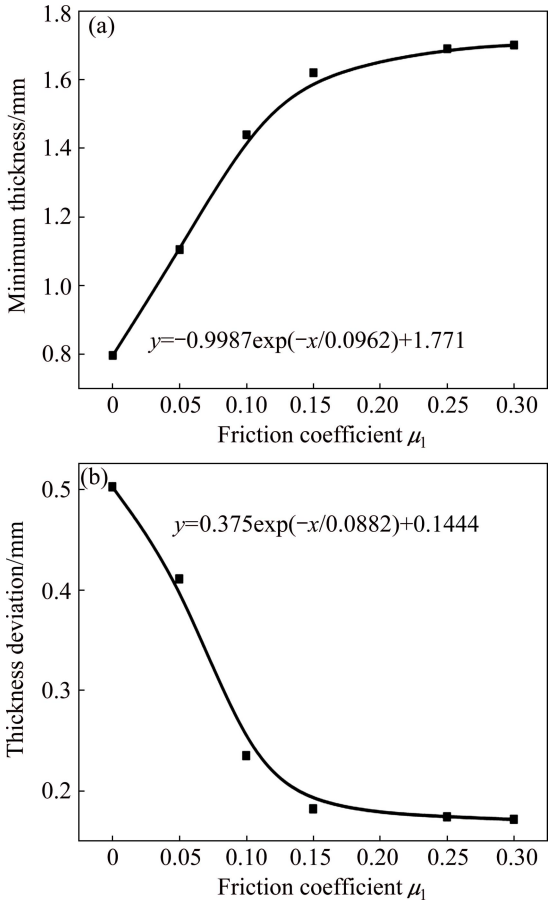

Fig. 8 Relationship between friction coefficient μ_1 and minimum thickness (a) and thickness deviation (b) under condition 2

Figure 8(b) presents the relationship between the thickness deviation and the friction coefficient μ_1. The thickness deviation decreases as the friction coefficient μ_1 increases. As the friction coefficient μ_1 is 0, the thickness deviation value is 0.5 mm, which indicates a severely uneven cup wall thickness distribution. The thickness deviation value is 0.17 mm at the friction coefficient μ_1 of 0.30. The thickness deviation markedly reduces at friction coefficient μ_1 lower than 0.15. Above 0.15, the thickness deviation decreases smoothly. Therefore, larger friction coefficient μ_1 results in better formability.

Figure 9 shows the strain path (dashed line) tracing the failure element during the drawing process with the friction coefficient μ_1 of 0. As shown, the failure is caused by the equal biaxial stretch at the center of the cup bottom, i.e., the major strain of the element is equal to the minor strain. The experimental part (left portion of Fig. 9) shows a large crack at the cup bottom. In actual experiment, the high temperature resistant lubricant B was painted on the punch surface to provide a low friction coefficient between the blank and the punch. In the forming process, the material of the cup bottom area is exposed to biaxial stretching. The material can be easily dragged to slide past the punch corner, when the friction coefficient between blank and punch is low, leading to considerable thinning. Thus, the friction force between the blank and the punch should be increased to a certain extent to obtain a good formability.

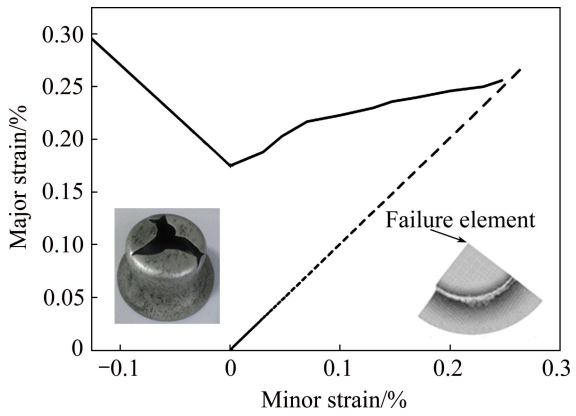

Fig. 9 Strain path of failure element under condition 2

4.3 Effect of friction coefficient μ_2

Under condition 3, the friction coefficient between the blank and the punch is kept constant as 0.20 and the friction coefficient between the blank and the holder, and the die is defined as μ_2, which varies from 0 to 0.30. The thickness distribution with the different friction coefficients μ_2 is illustrated in Fig. 10.

The thickness variation in Fig. 10 is similar to that in Fig. 3. However, the thickness distribution of the cup bottom is more sensitive to friction coefficient compared with that in Fig. 3. The cup bottom thickness markedly reduces as the friction coefficient μ_2 increases. The minimum thickness occurs near cup corner. The thickness thickens gradually in the sidewall region and flange region. As the friction coefficient μ_2 increases, the constrained force applied to the blank increases, which leads to severe unevenness of thickness distribution and elongation of the part.

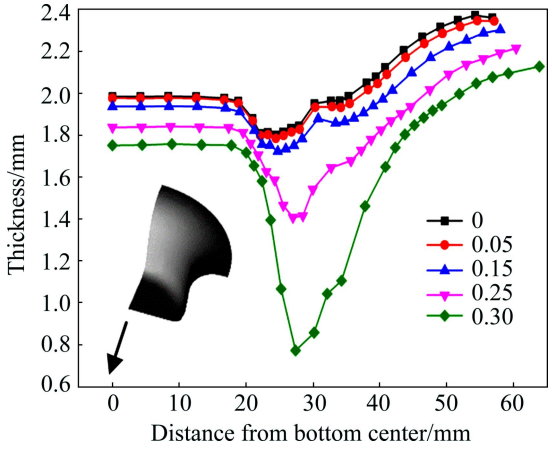

Fig. 10 Thickness distribution with various friction coefficients μ_2 under condition 3

Figure 11(a) displays the relationship between the minimum thickness and the friction coefficient μ_2. The minimum thickness decreases as the friction coefficient μ_2 increases. The minimum thickness gradually reduces first when the friction coefficient μ_2 is lower than 0.15, and then, it significantly decreases. A minimum thickness of 0.77 mm with a maximum thinning rate of as high as 61.5% was obtained at the friction coefficient μ_2 of 0.30. The relationship between the thickness deviation and the friction coefficient μ_2 is shown in Fig. 11(b). The thickness deviation gradually decreases first and then sharply increases as the friction coefficient μ_2 increases. The lowest thickness deviation (0.172 mm) was obtained at the friction coefficient μ_2 of 0.15, which indicates that the thickness was uniformly distributed.

Figure 12 demonstrates the strain path (dashed line) tracing the excessive thinning element when the friction coefficient μ_2 is 0.30. The strains of failure element are shown in stretch mode, i.e., the right-hand side of the FLD, which is different from that in Fig. 6. Moreover, the minor strain is less than major strain, which is attributed to the large radial stress and small circumferential stress of the failure element.

4.4 Experimental validation

Considering the effects of friction coefficient on the minimum thickness and thickness deviation under three conditions mentioned above comprehensively, the optimum friction coefficient is chosen as 0.15 for any

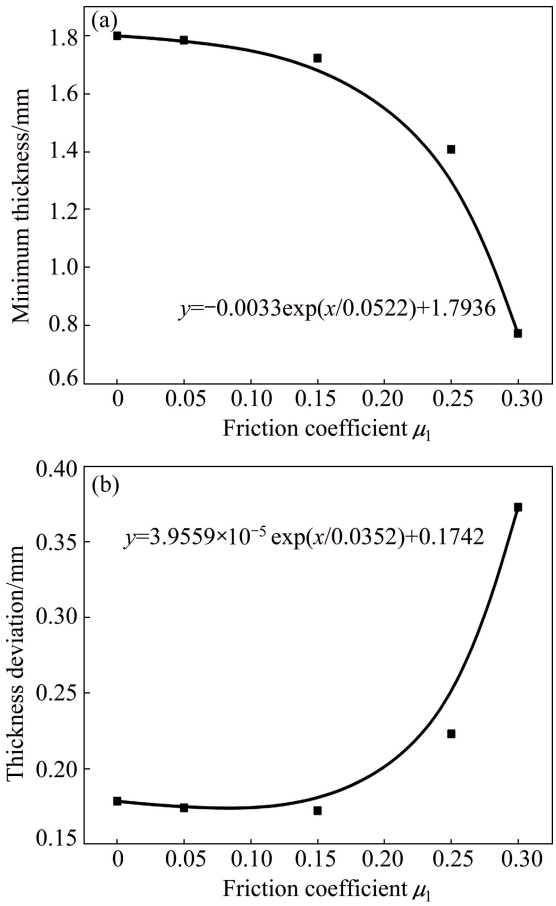

Fig. 11 Relationship between friction coefficient μ_2 and minimum thickness (a) and thickness deviation (b) under condition 3

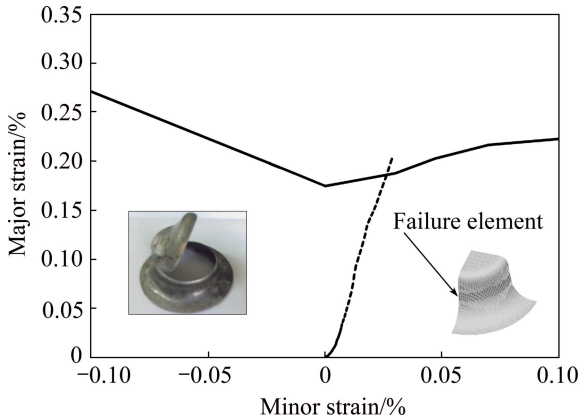

Fig. 12 Strain path of failure element under condition 3

interaction. The actual product was formed with high temperature resistant lubricant, which enables the friction coefficient to be about 0.15. To demonstrate the validity of the finite element analysis, the deformed shape and thickness distribution acquired from the FE simulation with friction coefficient of 0.15 for any interaction are compared with the actual cup formed in experiment.

As shown in Fig. 13, the cup geometries (left) obtained from FE simulation shows good consistency with those of the experimental one (right). The thickness distribution also demonstrates great agreement with the experimental data. The comparison fully reveals the predictive capability of the FE model.

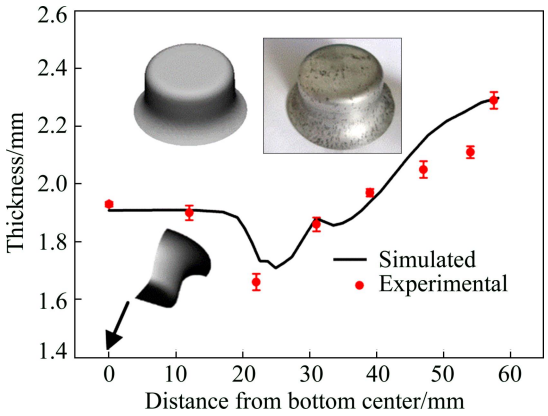

Fig. 13 Comparison of experimental and simulated results

5 Fracture analyses

As mentioned above, the crack generally happens at the bottom of the cup or near the cup corner. SEM was used to observe the fracture surfaces of the part to obtain a deep understanding on fracture mechanism. Two typical examples were provided and analyzed as follows.

The piece cut from the cup bottom is shown in Fig. 14(a). The small piece in the left corner of the figure was used for SEM observation after careful cleaning.

Figure 14 shows the fracture surface of the sample. Many equal-axis ductile dimples were observed in the figure, which is an obvious example of ductile fracture.

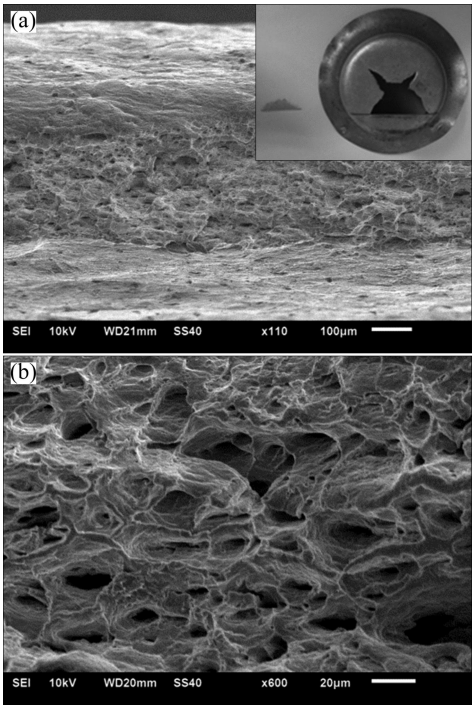

Fig. 14 Fracture surface of sample cut from cup bottom

The dimples formed in the plastic forming period prior to the complete crack. The dimples are like cups with upward edges. The coalescences of some adjacent voids can also be captured. After coalescence, a larger void formed. The ductile fracture originates from void nucleation, growth and coalescence, which is attributed to the equal axial tensile stress of material at the bottom of the cup. At the same time, at higher temperature, the atom vibrations have much greater frequency and the yield strength becomes lower. So much plastic deformation will be caused prior to fracture, and the fracture becomes more ductile naturally.

The sample cut from crack edge near the cup corner is illustrated in Fig. 15(a). The piece was carefully cleaned and used for SEM scanning.

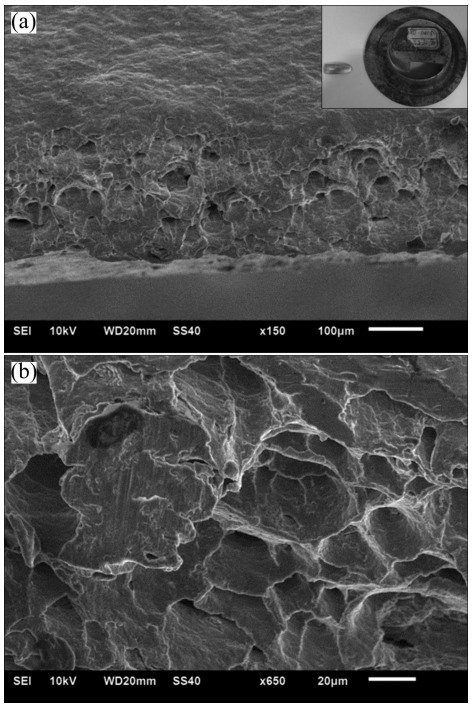

Fig. 15 Fracture surface of sample cut from cup corner

The SEM micrographs are shown in Fig. 15, which are different from those in Fig. 14. The ductile voids are caused by stretching apart near the outside of the blank and then, the blank was split to the other side, as the voids are in the same direction. The cleavage planes shown in Fig. 15 indicate the brittle fracture. At the end of deformation, thinning occurs near the cup corner in drawing process and the blank necks down to nearly a line. Then the crack first occurs near the outside surface of the blank and then rapidly extends to the inside surface. It is the ductile−brittle mixed fracture.

6 Conclusions

1) The friction coefficient significantly affects the formability, including the minimum thickness, the thickness deviation and the failure mode, during the deep drawing of aluminum alloy at elevated temperatures.

2) Under condition 1, the minimum thickness decreases and thickness deviation first decreases and then increases, as the friction coefficient μ_0 increases. The failure element occurs near the punch corner and the failure mode is the draw mode.

3) Under condition 2, the minimum thickness increases and thickness deviation decreases, as the friction coefficient μ_1 increases. The fracture happens at the center of the cup bottom and the failure mode is the equi-biaxial stretch mode.

4) Under condition 3, the minimum thickness decreases and thickness deviation first decreases and then increases, as the friction coefficient μ_2 increases. The excessive thinning occurs near the cup corner and the failure mode is the stretch mode.

5) For any of the conditions mentioned above, when the friction coefficient is 0.15, the formability is acceptable. Moreover, the simulated and the experimental results show good agreement.

6) The crack that happens at the center of cup bottom is the typical ductile fracture, whereas the crack near the cup corner is the ductile−brittle mixed fracture.

7) In the FE models, the friction coefficients are generally assumed constant during forming process. However, the friction coefficient varies in actual conditions depending on many factors, such as pressure, temperature and lubricant conditions. From a scientific standpoint, further research should better focus more on the relationship between friction coefficient and other forming parameters during hot drawing.

Acknowledgements

Authors would also like to sincerely thank the guidance and help from Professor Jian-guo LIN, Royal Academy of Engineering and Department of Mechanical Engineering, Imperial College, UK.

References

[1] HOSSAIN M M, HONG S T, PARK K Y, NA Y S. Microforming of superplastic 5083 aluminum alloy [J]. Transactions of Nonferrous Metals Society of China, 2012, 22(S): s656−s660.

[2] QUE Zhong-ping, MA Teng, WANG Jian, CHEN Jin, WANG Cai-hong, CHENG Wei-li. Microstructure and mechanical properties of as-cast Mg−8Sn−1Al−1Zn−xNi alloys [J]. Journal of Central South University, 2014, 21(9): 3426−3433.

[3] HIRSCH J. Recent development in aluminium for automotive applications [J]. Transactions of Nonferrous Metals Society of China, 2014. 24(7): 1995−2002.

[4] HIRSCH J, AL-SAMMAN T. Superior light metals by texture engineering: Optimized aluminum and magnesium alloys for automotive applications [J]. Acta Materialia, 2013, 61(3): 818−843.

[5] WANG Hui, LUO Ying-bing, FRIEDMAN P, CHEN Ming-he, GAO Lin. Warm forming behavior of high strength aluminum alloy AA7075 [J]. Transactions of Nonferrous Metals Society of China, 2012, 22(1): 1−7.

[6] FU L, WANG B, MENG Q, ZHOU J, LIN J. Factors affecting quality in hot stamping of aluminum alloy [J]. Journal of Central South University: Science and Technology, 2013, 44(3): 936−941. (in Chinese)
[7] CHO H, CHO J. Damage and penetration behavior of aluminum foam at various impacts [J]. Journal of Central South University, 2014, 21(9): 3442−3448.
[8] ZHONG H, ROMETSCH P, ESTRIN Y. Effect of alloy composition and heat treatment on mechanical performance of 6xxx aluminum alloys [J]. Transactions of Nonferrous Metals Society of China, 2014, 4(7): 2174−2178.
[9] KIM H S, KOC M, NI J. Development of an analytical model for warm deep drawing of aluminum alloys [J]. Journal of Material Processing Technology, 2008, 197(1−3): 393−407.
[10] BATE P S, RIDLEY N, ZHANG B, DOVER S. Optimisation of the superplastic forming of aluminium alloys [J]. Journal of Materials Processing Technology, 2006, 177(1−3): 91−94.
[11] ZHANG Pan, YE Ling-ying, ZHANG Xin-ming, GU Gang, JIANG Hai-chun, WU Yu-long. Grain structure and microtexture evolution during superplastic deformation of 5A90 Al−Li alloy [J]. Transactions of Nonferrous Metals Society of China, 2014, 24(7): 2088−2093.
[12] MOHAMED M, FOSTER A, LIN J. Solution heat treatment in HFQ process [J]. Steel Research International, 2008, 79(11): 160−167.
[13] TAKUDA H, MORI K, MASUDA I, ABE Y, MATSUO M. Finite element simulation of warm deep drawing of aluminium alloy sheet when accounting for heat conduction [J]. Journal of Material Processing Technology, 2002, 120(1−3): 412−418.
[14] BARIANI P F, BRUSCHI S, GHIOTTI A, MICHIELETTO F. Hot stamping of AA5083 aluminium alloy sheets [J]. CIRP Annals-Manufacturing Technology, 2013, 62(1): 251−254.
[15] ZHOU J, WANG B Y, LIN J G, FU L. Optimization of an aluminum alloy anti-collision side beam hot stamping process using a multi-objective genetic algorithm [J]. Archives of Civil and Mechanical Engineering, 2013, 13(3): 401−411.
[16] FAN X, HE Z, YUAN S, ZHENG K. Experimental investigation on hot forming–quenching integrated process of 6A02 aluminum alloy sheet [J]. Materials Science and Engineering A, 2013, 573: 154−160.
[17] MOHAMED M S, FOSTER A D, LIN J, BALINT D S, DEAN T A. Investigation of deformation and failure features in hot stamping of AA6082: Experimentation and modelling [J]. International Journal of Machine Tools and Manufacture, 2012, 53(1): 27−38.
[18] BROWNE M, HILLERY M. Optimising the variables when deep-drawing CR 1 cups [J]. Journal of Material Processing Technology, 2003, 136(1): 64−71.
[19] PADMANABHAN R, OLIVERIA M C, ALVES J L, MENEZES L F. Influence of process parameters on the deep drawing of stainless steel [J]. Finite Element in Analysis and Design, 2007, 43(14): 1062−1067.
[20] RAJU S, GANESAN G, KARTHIKEYAN R. Influence of variables in deep drawing of AA 6061 sheet [J]. Transactions of Nonferrous Metals Society of China, 2010, 20(10): 1856−1862.
[21] MENG Qing-lei. Research on hot stamping process of AA6111 [D]. Beijing: University of Science and Technology Beijng, 2011: 27−52. (in Chinese)
[22] FU Lei. Investigation of hot deformation behavior and hot stamping process of 6111 aluminum alloy [D]. Beijing: University of Science and Technology Beijng, 2013: 54−82. (in Chinese)
[23] YANAGIDA A, AZUSHIMA A. Evaluation of coefficients of friction in hot stamping by hot flat drawing test [J]. CIRP Annals-Manufacturing Technology, 2009, 58(1): 247−250.
[24] CHEMIN F R A, MARCONDES P V P. True strain distribution profile on sheet metal using different punch geometries [J]. Journal of the Brazilian Society of Mechanical Sciences and Engineering, 2008, 30(1): 1−6.
[25] PARK K, KIM Y. The effect of material and process variables on the stamping formability of sheet materials [J]. Journal of Material Processing Technology, 1995, 51(1): 64−78.
[26] JAISINGH A, NARASIMHAN K, DATE P, MAITI S, SINGH U. Sensitivity analysis of a deep drawing process for miniaturized products [J]. Journal of Material Processing Technology, 2004, 147(3): 321−327.
[27] COLGAN M, MONAGHAN J. Deep drawing process: Analysis and experiment [J]. Journal of Material Processing Technology, 2003, 132(1−3): 35−41.
[28] CHEN F K, HUANG T B, CHANG C K. Deep drawing of square cups with magnesium alloy AZ31 sheets [J]. International Journal of Machine Tools and Manufacture, 2003, 43(15): 1553−1559.
[29] CHOW C L, YU L G, TAI W H, DEMERI M Y. Prediction of forming limit diagrams for AL6111-T4 under non-proportional loading [J]. International journal of mechanical sciences, 2001, 43(2): 471−486.

摩擦因数对 AA6111 铝合金热冲压的影响

马闻宇[1]，王宝雨[1]，傅 垒[2]，周 靖[1]，黄鸣东[1]

1. 北京科技大学 机械工程学院，北京 100083；
2. 苏州有色金属研究院，苏州 215026

摘 要：通过有限元分析和试验的方法分三种情况研究了摩擦因数对 AA6111 铝合金热冲压筒形件的影响。结果表明，摩擦因数和润滑位置对铝合金热冲压成形件的最小厚度、厚度均匀性和失效形式影响显著。热冲压过程中，由于不同的润滑条件，试件的失效形式主要有拉−压失效、拉−拉失效和等双拉失效。基于对成形性的考虑，摩擦因数的最优值为 0.15。同时，有限元仿真和试验结果具有较高的一致性。破裂通常发生在筒形件底部中心和底部圆角附近，断裂形式分别为韧性断裂和韧性脆性混合断裂。

关键词：铝合金；冲压；摩擦因数；成形性；断口表面

(Edited by Yun-bin HE)